Article

Expression and Characterization of a Dye-Decolorizing Peroxidase from *Pseudomonas Fluorescens* Pf0-1

Nikola Lončar [1,2,*], Natalija Drašković [3], Nataša Božić [4], Elvira Romero [2,†], Stefan Simić [3], Igor Opsenica [3], Zoran Vujčić [3] and Marco W. Fraaije [2]

[1] GECCO Biotech, Nijenborgh 4, 9747AG Groningen, The Netherlands
[2] Molecular Enzymology group, University of Groningen, Nijenborgh 4, 9747AG Groningen, The Netherlands; elvira.romero@astrazeneca.com (E.R.); m.w.fraaije@rug.nl (M.W.F.)
[3] Faculty of Chemistry, University of Belgrade, Studentski trg 12-16, 11000 Belgrade, Serbia; draskovic.natalija@gmail.com (N.D.); ssimic@chem.bg.ac.rs (S.S.); igorop@chem.bg.ac.rs (I.O.); zvujcic@chem.bg.ac.rs (Z.V.)
[4] ICTM-Center of Chemistry, University of Belgrade, Studentski trg 12-16, 11000 Belgrade, Serbia; nbozic@chem.bg.ac.rs
* Correspondence: n.loncar@rug.nl
† Current address: AstraZeneca R&D Gothenburg, Discovery Sciences, S-431 83 Mölndal, Sweden.

check for updates

Abstract: The consumption of dyes is increasing worldwide in line with the increase of population and demand for clothes and other colored products. However, the efficiency of dyeing processes is still poor and results in large amounts of colored effluents. It is desired to develop a portfolio of enzymes which can be used for the treatment of colored wastewaters. Herein, we used genome sequence information to discover a dye-decolorizing peroxidase (DyP) from *Pseudomonas fluorescens* Pf-01. Two genes putatively encoding for DyPs were identified in the respective genome and cloned for expression in *Escherichia coli*, of which one (*Pf*DyP B2) could be overexpressed as a soluble protein. *Pf*DyP B2 shows some typical features known for DyPs which includes the ability to convert dyes at the expense of hydrogen peroxide. Interestingly, *t*-butyl hydroperoxide could be used as an alternative substrate to hydrogen peroxide. Immobilization of *Pf*DyP B2 in calcium-alginate beads resulted in a significant increase in stability: *Pf*DyP B2 retains 80% of its initial activity after 2 h incubation at 50 °C, while the soluble enzyme is inactivated within minutes. *Pf*DyP B2 was also tested with aniline and ethyl diazoacetate as substrates. Based on GC-MS analyses, 30% conversion of the starting material was achieved after 65 h at 30 °C. Importantly, this is the first report of a DyP-catalyzed insertion of a carbene into an N-H bond.

Keywords: DyP peroxidase; oxidoreductase; reactive dye; decolorization

1. Introduction

Peroxidases are oxidoreductases involved in a variety of biochemical processes, including the biosynthesis of cell wall material and immunological host-defense responses [1]. The recently discovered DyP-type peroxidases (DyPs, dye-decolorizing peroxidases; EC 1.11.1.19) represent a novel superfamily of heme-containing enzymes. They share no significant similarity in primary sequence or structure to other peroxidase superfamilies [2]. DyPs possess a broad substrate specificity and low pH optimum [2], while they are most stable at neutral pH [3]. Using hydrogen peroxide as an electron acceptor, they are capable of catalyzing efficient oxidations of a wide array of industrially relevant substrates including dyes with anthraquinone structure, *β*-carotene, and aromatic sulfides [4–8]. Instead of a distal histidine

acting as an acid-base catalyst, DyPs contain an aspartate active site residue within a highly conserved GXXDG distal motif [8], although recent findings indicate that instead of aspartate some DyPs have a glutamate [9]. On the proximal side, the heme iron of DyPs is coordinated by a histidine.

Several bacterial DyPs were found to be robust enzymes and thus potent biocatalysts [10–12]. Since they can degrade a variety of synthetic dyes, DyPs can potentially be used in the bioremediation of dye-contaminated waste water. Two fungal DyP-type peroxidases were shown to degrade *β*-carotene [7], which is of tremendous interest in the food industry for enabling the enzymatic whitening of whey-containing foods and beverages. DyP peroxidases also show promise as novel anti-microbial (pro)drug targets [13]. Their myriad industrial uses point to the importance of discovery and characterization of these enzymes.

In this work, we have used the available genome sequence of *Pseudomonas fluorescens* Pf0-1 to identify a gene coding for a DyP (*Pf*DyP B2). This peroxidase has been overexpressed in *Escherichia coli* and purified. It shows activity towards various substrates including 2,6-dimethoxyphenol, 2,2′-Azino-bis(3-ethylbenzothiazoline-6-sulfonic acid) (ABTS), *o*-dianisidine, and reactive dyes. Besides hydrogen peroxide, *Pf*DyP B2 was able to use *t*-butyl hydroperoxide as an electron acceptor. *Pf*DyP B2 was also probed for a reaction that was recently reported to be catalyzed by several heme-containing proteins including cytochrome P450 monooxygenases and myoglobin: carbonyl-olefination, cyclopropanation, and N/S-H insertion reactions using the reaction of ethyl diazoacetate with heme under anaerobic conditions [14–17]. Recently, it was also shown that a DyP, YfeX from *E. coli*, is able to perform carbonyl olefination [18]. YfeX was initially reported to be a deferrochelatase, extracting iron ions from heme [19]. However, it was later identified as a DyP [20,21]. Another recent study on the implementation of YfeX in the synthesis of tryptamine precursors [22] triggered our attention to investigate whether *Pf*DyP B2 can be similarly used as a hemoprotein scaffold for reactions not probed before using a DyP. Our work shows that the reaction between aniline and ethyl diazoacetate can be satisfactorily achieved using *Pf*DyP B2 as a biocatalyst. Remarkably, this is the first report of a DyP-catalyzed insertion of a carbene into an N-H bond.

2. Results

2.1. Expression and Purification

A search for DyP peroxidases in the predicted proteome of *P. fluorescences* Pf-01 using RedoxiBase (http://peroxibase.toulouse.inra.fr/) revealed that this organism contains three peroxidases that belong to the DyP peroxidase superfamily, one of which belongs to clade A DyPs and two to clade B DyPs. In addition, one gene encoding a catalase-peroxidase (KatG) was identified. Clade A DyPs have been hypothesized to be less catalytically active due to a mixed spin state of the heme [23]. Two genes encoding for DyPs belonging to clade B were amplified by PCR using genomic DNA of *P. fluorescens* Pf-01 as a template. These fragments have been cloned into a pBAD vector and expression was carried out under different conditions. *Pf*DyP B1 could not be expressed in sufficient amounts (data not shown), while *Pf*DyP B2 was overexpressed and appeared as the most dominant protein band upon SDS-PAGE analysis of the cell-free extract (Figure 1a). The predicted molecular weight of *Pf*DyP B2 is 35 kDa. Purification of the cell free extract using Ni^{2+}-Sepharose showed that the binding of *Pf*DyP B2 to the resin was very poor since it eluted with less than 10 mM imidazole. This eluted fraction contained additional proteins hampering the biochemical characterization of PfDyP B2. Thus, further purification was performed. Mixed mode resins enable the purification of biomolecules without feedstream conditioning and can operate across a wide range of salt concentrations and pH. One of the mixed mode resins is Nuvia aPrime 4A (Bio Rad), which is designed with a positively charged hydrophobic ligand, which helps in biomolecule binding by both hydrophobic and anionic interactions. Therefore, Nuvia aPrime 4A mixed mode resin was used for polished purification of *Pf*DyP B2. Active peroxidase eluted with 1 M NaCl and showed ~95% purity upon SDS-PAGE analysis (Figure 1).

The purification procedure yielded ~35 mg of purified His-tagged *Pf*DyP B2 from 1 L of culture broth. This two-step workflow is readily scalable for process production.

Previous studies have shown that DyPs represent a novel peroxidase superfamily harboring a heme molecule in their structure [24,25]. A UV-Vis absorption spectrum of the purified enzyme was recorded between 250 and 750 nm. The Soret band at 405 nm (Figure 1b) indicates that the heme cofactor had indeed been incorporated into the purified PfDyP B2. The Reinheitzahl value (Rz, the ratio of A_{405}/A_{280}) for the purified enzyme was 1.16.
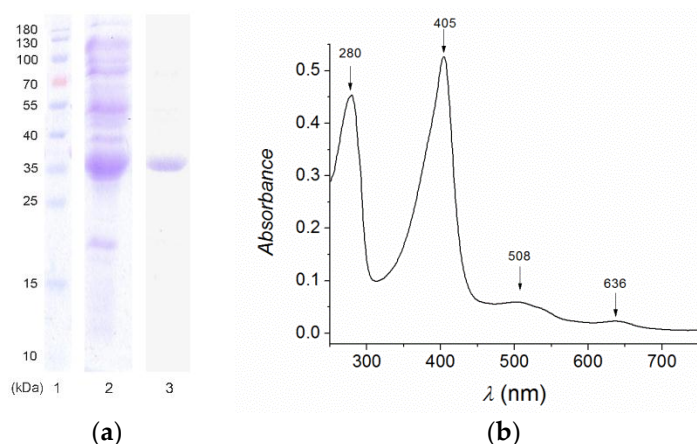

Figure 1. (**a**) SDS PAGE analysis. Lane 1: Molecular markers; lane 2: Cell free extract; lane 3: *Pf*DyP B2 fraction after purification with Nuvia aPrime 4A chromatography. (**b**) UV-Vis spectrum of *Pf*DyP B2.

2.2. Biochemical Characterization

The purified enzyme was most active at pH 4.0 (Figure 2) with moderate activity between pH 3.0 and 6.0, which is in perfect agreement with other studies on DyPs [9,23,26].
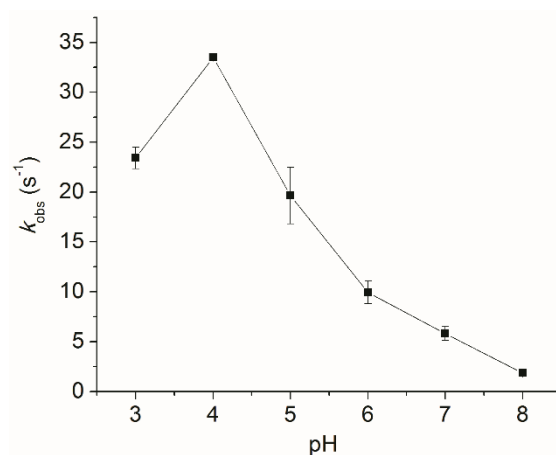

Figure 2. The effect of pH on the observed rate (k_{obs}) of oxidation of ABTS by *Pf*DyP B2.

The relative activity of the purified *Pf*DyP B2 enzyme was tested using 0.5 mM ABTS and 0.1 mM hydrogen peroxide in the presence of various cations (Ca^{2+}, Mg^{2+}, Zn^{2+}, Mn^{2+}, Co^{2+}, Fe^{2+}, and Hg^{2+}) and reducing agents (aminotriazole, EDTA, imidazole, DTT, Cys, and Na-azide). The results show that the relative activity was not diminished by the addition of Ca, Mg, Zn, Mn, and Co ions, but was significantly reduced in the presence of Fe and Hg ions (Figure 3a). Partial inhibition of the purified enzyme was observed with aminotriazole, EDTA, and imidazole, whereas almost complete inhibition was seen with DTT, Cys, and Na-azide (Figure 3b).
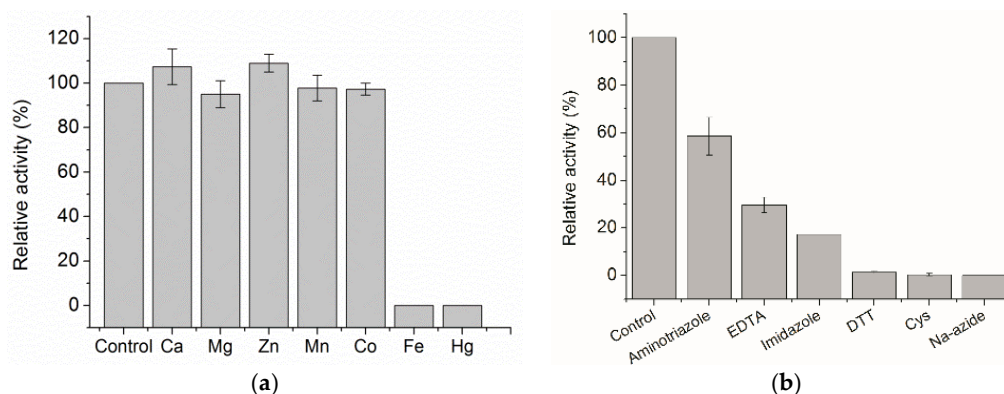
Figure 3. (**a**) The effect of metal ions on activity of *Pf*DyP B2. (**b**) The effect of inhibitors on the activity of *Pf*DyP B2. Activity in the absence of inhibitors was taken as 100%.

To investigate the substrate scope of the purified *Pf*DyP B2, it was tested using various well-known peroxidase substrates at ambient temperature. As shown in Table 1, *Pf*DyP B2 showed activity towards most of the assayed substrates including ABTS and aromatic, azo, and anthraquinone dyes. In addition, guaiacol, 2,6-dimethoxyphenol, manganese, veratryl alcohol, CBZ-ethanolamine, syringaldehyde, and acetosyringone were tested, but *Pf*DyP B2 was inactive towards them. The reactions were carried out in 50 mM Na-acetate buffer pH 4.0 for ABTS, *o*-dianisidine, and pyrogallol. In the case of reactive dyes, assays were carried out using 50 mM sodium-acetate buffer at pH 3.0 since a tenfold higher activity towards these dyes was observed at this pH value.

Table 1. Kinetic parameters measured for *Pf*DyP B2.

Substrate	λ (nm)	ε (mM^{-1}cm^{-1})	K_m (mM)	k_{cat} (s^{-1})
ABTS	414	36.6	0.22 ± 0.04	102 ± 6.2
o-Dianisidine	460	11.3	0.003 ± 0.001	14.7 ± 1.7
Pyrogallol	430	2.47	1.45 ± 0.63	1.98 ± 0.03
Reactive blue 4	610	4.2	0.010 ± 0.004	1.54 ± 0.13
Reactive black 5	597	37	0.006 ± 0.002	0.04 ± 0.01
H_2O_2 [a]	240	0.0394	0.52 ± 0.12	23 ± 0.84
t-BuOOH [a]	n.a.	n.a.	415 ± 144	97 ± 28

[a] Measured by using ABTS as substrate. n.a.- not applicable

Using Kraft lignin as a substrate, a Michaelis-Menten saturation curve was observed (Figure 4), similar to that previously observed for other DyPs [27,28].
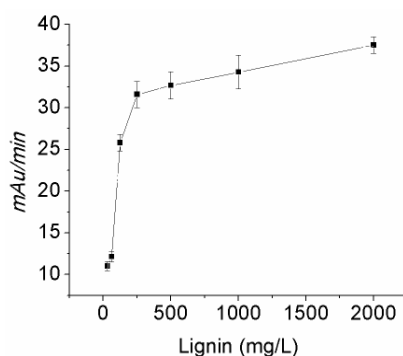

Figure 4. The steady-state activity of *Pf*DyP B2 with Kraft lignin as monitored by absorbance change at 465 nm [27,28].

*Pf*DyP B2 showed poor stability at 40 and 50 °C, being inactivated within minutes. However, its activity remained unaffected for at least 2 h at 30 °C. Among existing strategies for the improvement of

enzyme stability, a well-known approach is enzyme immobilization. Immobilization also offers the possibility to reuse the respective enzyme and allows easy separation of enzymes and product, which are factors influencing the overall cost of enzymatic industrial processes. *Pf*DyP B2 was immobilized in alginate by mixing an enzyme solution with 2% sodium-alginate followed by droplet ejection into a 2% CaCl$_2$ solution. The beads were left to age in the CaCl$_2$ solution followed by washing steps with buffer. Fifty percent of the enzyme leaked out of the beads according to activity and protein measurements. The remaining enzyme was retained in the beads. Immobilized *Pf*DyP B2 retained 80% of initial activity after a 2 h incubation at 50 °C, revealing a significant increase in stability compared to soluble enzyme.

Encouraged by previous reports of heme-containing enzymes catalyzing the insertion of carbenes into N-H bonds [15,17], a reaction between aniline and ethyl diazoacetate was investigated using *Pf*DyP B2 as a catalyst (Scheme 1). Aniline and ethyl diazoacetate were reacted in the presence of sodium dithionite as a reductant and 0.4 mol% enzyme, using acetate buffer, pH 4.5. The reaction was kept at 30 °C for 65 h. Subsequently, the product formation was analyzed and confirmed by GC-MS. Conversion of the starting material was determined to be 30%.

30% conversion (GC-MS)
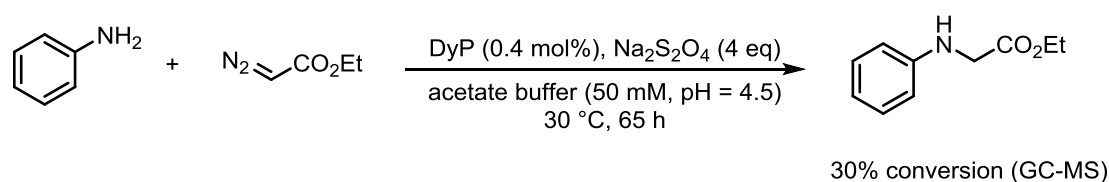
Scheme 1. The *Pf*DyP B2-catalyzed reaction between aniline and ethyl diazoacetate.

3. Discussion

Dye-decolorizing peroxidases can be useful biocatalysts for industrial applications due to their extraordinary ability to degrade a variety of synthetic dyes. They have the potential to be used for the bioremediation of dye-contaminated waste water. In the current study, we have purified a His-tagged DyP from *P. fluorescens* Pf-01 expressed in *E. coli*. Purification was performed on an IMAC resin which resulted in a partially pure target protein. A hydrophobic anion exchanger, Nuvia aPrime 4A, was used to obtain highly pure PfDyP B2. Although it was not tested in this particular instance, it may be that Nuvia aPrime 4A can provide a single-step purification directly from the crude cell extract. Conveniently this resin is compatible with high salt concentration and a broad pH range without the need for feed dilution/reconstitution. This would help in limiting the number of steps required to generate a highly pure enzyme sample. While IMAC is widely used for purification of recombinant proteins, mixed-mode resins should also be considered when it is not so straightforward to achieve a desired purity in one step by affinity chromatography.

The steady-state kinetic parameters determined for PfDyP B2 indicate that it is highly active on ABTS and *o*-dianisidine. This suggests that PfDyP B2 may be exploited for the biomedical applications and various assays which are typically based on the prototype plant peroxidase, horseradish peroxidase (HRP). Reactive blue 4 is oxidized by PfDyP B2 at a similar rate to pyrogallol, while Reactive black 5 is a more recalcitrant dye (Table 1).

Inactivation by hydrogen peroxide is often underlined as the weakness of peroxidases when it comes to industrial application. However, it is also known that this problem can be solved by using alternative electron acceptors [29]. Interestingly, beside hydrogen peroxide, *Pf*DyP B2 was able to use *t*-butyl hydroperoxide as an electron acceptor. The k_{cat} value using this compound is four-fold higher than when using hydrogen peroxide. However, the K_m for *t*-butyl hydroperoxide is quite high which is limiting the possibility of using it in wastewater treatment. While *t*-butyl hydroperoxide is a more expensive electron acceptor than hydrogen peroxide, it may still offer some advantages. The use of *t*-butyl hydroperoxide can reduce the overall enzyme loading in the process since enzyme inactivation by hydrogen peroxide will be minimized. This is something that would have to be optimized case by

case though reaction engineering and is process-dependent. In large-scale industrial processes, such as dye decolorization, the use of *t*-butyl hydroperoxide is probably not feasible. However, DyPs may also be used in some other applications, for example for the production of high-value chemicals, as described for *Tfu*DyP for enantioselective sulfoxidation [8]. The acceptance of *t*-butyl hydroperoxide by the enzyme also discloses mechanistic information; apparently, this organic oxidant is able to reach the heme while this is not the case for all peroxidases.

Prior studies have also shown that DyP-type peroxidases can act on lignin and can be involved in its degradation [30]. Enzymatic lignin depolymerization is highly attractive, as it offers access to a wide array of aromatic precursors which can be further functionalized for the production of high-added value chemicals. We tested if *Pf*DyP B2 can act on Kraft lignin. As shown in Figure 4, we detected an increased DyP activity with an increase in the Kraft lignin concentration. Other DyPs acting on lignin and originating from *Pseudomonas* sp. are described in the literature, giving further confirmation of the potential of *Pf*DyP B2 for lignin valorization [31]. One must keep in mind that the lignin depolymerization process is very complicated and will hardly be achieved by one enzyme. Considering the radical mechanism of laccases and peroxidases it is certain that the concerted action of several enzymes or trapping of produced radicals is needed to achieve depolymerization. Otherwise, depolymerization and repolymerization will occur, as demonstrated in recent publications of synthesis of lignin oligomers [11,32].

Any scale up of enzymatic processes is still highly dependent on the cost of enzymes. Joint efforts of increasing the expression levels and the efficient use of enzymes are needed to make the process economically feasible. Our first attempts at the immobilization of *Pf*DyP B2 have demonstrated that this approach is clearly beneficial. The immobilized enzyme was able to withstand increased temperature as compared to its soluble counterpart. Magnetic particles may further aid and improve the activity of DyPs as shown recently for a similar DyP from *P. fluorescens* Pf-5 [33].

Except for valorising lignin by using DyPs, these heme-containing enzymes may also be used for non-natural reactions. Recent papers have shown that hemoproteins can be used for a number of attractive reactions [14–17]. This study shows that *Pf*DyP B2 can be used to perform an insertion of a carbene in an N-H bond. To our knowledge, this is the first time that a DyP was able to catalyze such a reaction.

4. Materials and Methods

4.1. Reagents and Enzymes

Pfu polymerase, restriction enzymes, and prestained protein ladders were from Thermo Scientific. Ni^{2+}-Sepharose HP was from GE Lifescience. All other chemicals were supplied by Sigma-Aldrich (St. Louis, MO, USA) and were of analytical grade.

4.2. Strains, Plasmids, and Growth Conditions

The *E. coli* strain TOP10 was used for routine cloning and maintenance of all plasmid constructs. This strain was also used for overexpression of *Pf*DyP B1 and *Pf*DyP B2. The genes encoding *Pf*DyP B1 (RefSeq: YP_348895.1) and *Pf*DyP B2 (RefSeq: YP_348987.1) were amplified by polymerase chain reaction from genomic DNA of *P. fluorescens* Pf0-1. The PCR fragments were amplified using primers GAC GTA CAT ATG AGT TAC TAC CAG C and ATA GAA TTC GCC GAT GCG CAG T for *Pf*DyP B1 and ACT CAT ATG TTG GGA GTC ACG ATC AT and ATT GAA TTC TCG CTC TGC CAA CTC TT for *Pf*DyP B2 cloning between NdeI and EcoRI restriction sites of the pBADNdeIHis vector to give the pBAD-*Pf*DyP B1 and pBAD-*Pf*DyP B2 constructs for the expression of peroxidases with an C-terminal mycHis tag. Restriction sites in primers are underlined. pBad*NdeI*His is a pBAD/Myc-HisA-derived expression vector (Thermo Fisher, Waltham, MA, USA) in which the *NdeI* site has been removed and the *NcoI* site has been replaced by *NdeI*. For verification, all created constructs have been sequenced (GATC Biotech).

4.3. Sequence Analysis

The ProtParam tool at the ExPASy server (URL: http://web.expasy.org/protparam/) was used to calculate extinction coefficients for *Pf*DyPB1 ($36{,}440\ \mathrm{M^{-1}\ cm^{-1}}$) and *Pf*DyPB2 ($25{,}690\ \mathrm{M^{-1}\ cm^{-1}}$).

4.4. Expression and Purification

E. coli TOP10 cells expressing *Pf*DyPB1 and *Pf*DyPB2 were grown in LB medium at 37 °C to saturation overnight. The following day, cultures were diluted 1:100 into fresh media and grown until $OD_{600} = 1.25$ after which 0.02% L-arabinose and 0.75 mM hemin were added to induce the expression of *Pf*DyP B1 and B2, respectively. Expression was carried out at 30 °C, 180 rpm for 24 h. Cells were harvested by centrifugation at 6000 rpm and washed once with 50 mM potassium phosphate buffer pH 8.0 with 0.5 M NaCl. Pelleted cells were resuspended in the same buffer and disrupted by sonication. Cell-free extract was obtained after centrifugation at 11,000 rpm at 4 °C for 1 h.

For purification of His-tagged *Pf*DyP B2, cell free extract was loaded on a $\mathrm{Ni^{2+}}$-Sepharose HP column equilibrated with 50 mM potassium phosphate buffer pH 8.0 with 0.5 M NaCl. Non-specifically bound proteins were washed away stepwise with 2 column volumes of 10 mM imidazole in starting buffer followed by elution with 250 mM imidazole in the same buffer. *P. fluorescens* DyP shows poor binding to the column but elutes as an observable red-colored fraction. Collected fractions were analyzed by reducing SDS-PAGE and subsequent protein staining. Fractions containing DyP were impure and were further purified on Nuvia aPrime 4A resin from Bio-Rad Laboratories. Binding to the resin was achieved using potassium phosphate buffer 50 mM pH 7.8 and purification was carried out with stepwise elution using starting buffer with 0.1 M NaCl, 0.2 M NaCl, 0.3 M NaCl, 0.5 M NaCl, and 1.0 M NaCl. Active peroxidase elutes with 1.0 M NaCl and shows high purity on SDS-PAGE analysis. Pure fractions were pooled and concentrated using an Amicon stirring cell equipped with a 10 kDa cut-off membrane.

Protein fractions were analyzed by 10% SDS-PAGE using the SE260 Mighty Small II Deluxe System. The UV-Vis absorption spectra of purified DyPB were recorded between 200 and 800 nm using a Shimadzu UV-1800 spectrophotometer in 1 cm quartz cuvettes at room temperature.

4.5. Steady-State Kinetic Analyses

DyP activity was measured spectrophotometrically using Shimadzu UV-1800 at ambient temperature. The pH optimum for activity was determined using 0.5 mM ABTS and 1.0 mM H_2O_2 using a set of buffers (0.10 M of Na-acetate pH 3.0–5.0, MES pH 6.0, TrisHCl 7.0–8.0, and glycine/NaOH pH 9.0–10.0). Upon determination of the optimal pH, further measurements were made in an appropriate buffer.

Kinetic parameters of peroxidase activity (k_{cat} and K_m) were measured using different concentrations of ABTS, *o*-dianisidine, pyrogallol, Reactive blue 4, and Reactive black 5 with 1.0 mM H_2O_2 as co-substrate by adding 10 µL of suitably diluted enzyme (final concentration 5.3 nM). For H_2O_2 and *t*-butyl hydroperoxide, a fixed concentration of ABTS was used and the concentration of peroxide varied. Control reactions were included without using enzyme, H_2O_2, or both. Blanks were recorded in parallel with the measurements and subtracted accordingly. The kinetic parameters were calculated by fitting the data with a Michaelis-Menten equation using nonlinear analysis.

Kraft Lignin was tested as a substrate for *Pf*DyP B2 using a previously described procedure [27,28]. Briefly, Kraft lignin was dissolved in 0.10 M NaOH (10 mg/mL) and the pH was adjusted to 4.0 using 1.0 M sodium-acetate buffer. Different dilutions of this stock were mixed in 1 mL cuvette with *Pf*DyP B2 (25 µL, 1 mg/mL) and hydrogen peroxide (0.5 mM, final concentration), and the absorbance was monitored for 5 min at 465 nm. Inhibition of the peroxidase was tested using 3-amino-1,2,4-triazole, imidazole, DTT, cysteine, and sodium-azide. The enzyme was assayed for peroxidase activity as described above after preincubation with the inhibitor for 3 min prior to performing the assay with ABTS.

Thermal stability was determined by measuring residual activity upon incubating aliquots of *Pf*DyP B2 at 30 °C, 40 °C, and 50 °C. Samples were withdrawn at specific time points and activity was determined spectrophotometrically as described above.

4.6. Immobilization Study

*Pf*DyP B2 was immobilized in alginate by mixing 1 mL of enzyme solution (2 mg/mL) with 1 mL of 2% sodium-alginate followed by droplet ejection through a syringe needle into 1 L of 2% $CaCl_2$ solution, stirred using a mechanical overhead stirrer. The beads were left to age in the $CaCl_2$ solution followed by washing steps with buffer. The produced calcium alginate beads were collected and washed three times using 10 mL of 50 mM Na-acetate buffer pH 4.0. The leaking of *Pf*DyP B2 from alginate beads was checked in all wash fractions by measuring protein concentration using Bradford assay and activity of *Pf*DyP B2 using ABTS as substrate. The total protein amount in wash fractions was subtracted from the starting amount of *Pf*DyP B2 to estimate the amount of enzyme which was successfully entrapped in alginate beads. The immobilized enzyme was tested for activity using the ABTS assay before and after incubation in a water bath set at 50 °C.

4.7. Procedure for the DyP-Catalyzed Reaction Between Aniline and Ethyl Diazoacetate

The reaction was carried out in a 2 mL glass vial (Agilent Technologies, San Diego, CA, USA). To an unsealed vial charged with argon and a stirring bar, 840 μL of a 47 μM solution of DyP in acetate buffer (50 mM, pH = 4.5) was added. The vial was sealed with a silicone septum and the headspace of the vial was flushed with argon. A 1 M solution of sodium dithionite in acetate buffer (50 mM, pH 4.5) was degassed by bubbling with argon for 5 min, and 40 μL of this solution was added to the reaction mixture via a glass syringe. Solutions of ethyl diazoacetate and aniline were degassed in the same fashion prior to addition to the reaction mixture. Subsequently, 20 μL of a 0.5 M ethyl diazoacetate solution in a 1:1 (*v/v*) mixture of acetate buffer and dimethyl sulfoxide, and 100 μL of a 0.1 M solution of aniline in acetate buffer were added in the indicated order. The final concentrations of the added compounds were: 10 mM aniline, 10 mM ethyl diazoacetate, 40 mM sodium dithionite, and 40 μM DyP. The reaction mixture was stirred on a magnetic stirrer at 30 °C for 65 h. After the elapsed time, the mixture was extracted with ethyl acetate, dried over sodium sulfate, concentrated under reduced pressure, and analyzed by GC-MS.

GC-MS spectra (Supplementary Materials) of the synthesized compound were acquired on an Agilent Technologies 7890A apparatus equipped with a DB-5 MS column (30 m × 0.25 mm × 0.25 μm), a 5975C MSD and FID detector. The selected values are as follows: carrier gas was He (1.0 mL/min), temperature linearly increased from 40–315 °C (10 °C/min), injection volume: 1 μL, temperature: 250 °C, temperature (FID detector): 300 °C. CI was used as the ion source, with isobutane as the reagent gas. The mass spectrum was collected after a 4 min solvent delay.

5. Conclusions

*Pf*DyP B2 is an enzyme which can be easily expressed and used in peroxidase-based applications, ranging from assays and biosensors to dye-contaminated wastewater treatments. Notably, the first DyP-catalyzed insertion of a carbene into an N-H bond was reported. Although this is a preliminary result it could be a good platform for future applications of *Pf*DyP B2 in the synthesis of valuable compounds.

Supplementary Materials: The following are available online at http://www.mdpi.com/2073-4344/9/5/463/s1, GC-MS spectra of the synthesized compound.

Author Contributions: Conceptualization, N.L. and N.B.; methodology, N.L.; investigation, N.L., N.D., E.R., S.S., I.O., and N.B.; resources, M.F. and Z.V.; writing—original draft preparation, N.L.; writing—review and editing, all authors.

Conflicts of Interest: The authors declare no conflict of interest.

References

1. Fraaije, M.W.; Bloois, E.V. DyP-type peroxidases: A promising and versatile class of enzymes. *Enzym. Eng.* **2012**, *1*, 1–3. [CrossRef]
2. Colpa, D.I.; Fraaije, M.W.; van Bloois, E. DyP-type peroxidases: A promising and versatile class of enzymes. *J. Ind. Microbiol. Biotechnol.* **2014**, *41*, 1–7. [CrossRef] [PubMed]
3. Lončar, N.; Colpa, D.I.; Fraaije, M.W. Exploring the biocatalytic potential of a DyP-type peroxidase by profiling the substrate acceptance of *Thermobifida fusca* DyP peroxidase. *Tetrahedron* **2016**, *72*, 7276–7281. [CrossRef]
4. Liers, C.; Bobeth, C.; Pecyna, M.; Ullrich, R.; Hofrichter, M. DyP-like peroxidases of the jelly fungus *Auricularia auricula-judae* oxidize nonphenolic lignin model compounds and high-redox potential dyes. *Appl. Microbiol. Biotechnol.* **2010**, *85*, 1869–1879. [CrossRef]
5. Linde, D.; Ruiz-Duenas, F.J.; Fernandez-Fueyo, E.; Guallar, V.; Hammel, K.E.; Pogni, R.; Martinez, A.T. Basidiomycete DyPs: Genomic diversity, structural-functional aspects, reaction mechanism and environmental significance. *Arch. Biochem. Biophys.* **2015**, *574*, 66–74. [CrossRef]
6. Salvachua, D.; Prieto, A.; Martinez, A.T.; Martinez, M.J. Characterization of a novel dye-decolorizing peroxidase (DyP)-type enzyme from *Irpex lacteus* and its application in enzymatic hydrolysis of wheat straw. *Appl. Environ. Microbiol.* **2013**, *79*, 4316–4324. [CrossRef] [PubMed]
7. Scheibner, M.; Hulsdau, B.; Zelena, K.; Nimtz, M.; de Boer, L.; Berger, R.G.; Zorn, H. Novel peroxidases of *Marasmius scorodonius* degrade beta-carotene. *Appl. Microbiol. Biotechnol.* **2008**, *77*, 1241–1250. [CrossRef]
8. van Bloois, E.; Torres Pazmino, D.E.; Winter, R.T.; Fraaije, M.W. A robust and extracellular heme-containing peroxidase from *Thermobifida fusca* as prototype of a bacterial peroxidase superfamily. *Appl. Microbiol. Biotechnol.* **2010**, *86*, 1419–1430. [CrossRef]
9. Habib, M.H.; Rozeboom, H.J.; Fraaije, M.W. Characterization of a new DyP-Peroxidase from the alkaliphilic cellulomonad, *Cellulomonas bogoriensis*. *Molecules* **2019**, 24. [CrossRef]
10. Colpa, D.I.; Lončar, N.; Schmidt, M.; Fraaije, M.W. Creating Oxidase-Peroxidase Fusion Enzymes as a Toolbox for Cascade Reactions. *ChemBioChem* **2017**, *18*, 2226–2230. [CrossRef]
11. Habib, M.H.M.; Deuss, P.J.; Lončar, N.; Trajkovic, M.; Fraaije, M.W. A biocatalytic one-pot approach for the preparation of lignin oligomers using an oxidase/peroxidase cascade enzyme system. *Adv. Synth. Catal.* **2017**, *359*, 3354–3361. [CrossRef]
12. Yu, W.; Liu, W.; Huang, H.; Zheng, F.; Wang, X.; Wu, Y.; Li, K.; Xie, X.; Jin, Y. Application of a novel alkali-tolerant thermostable DyP-type peroxidase from *Saccharomonospora viridis* DSM 43017 in biobleaching of eucalyptus kraft pulp. *PLoS ONE* **2014**, *9*, e110319. [CrossRef] [PubMed]
13. Kong, L.; Guo, D.; Zhou, S.; Yu, X.; Hou, G.; Li, R.; Zhao, B. Cloning and expression of a toxin gene from *Pseudomonas fluorescens* GcM5-1A. *Arch. Microbiol.* **2010**, *192*, 585–593. [CrossRef] [PubMed]
14. Coelho, P.S.; Brustad, E.M.; Kannan, A.; Arnold, F.H. Olefin cyclopropanation via carbene transfer catalyzed by engineered cytochrome P450 enzymes. *Science* **2013**, *339*, 307–310. [CrossRef] [PubMed]
15. Wang, Z.J.; Peck, N.E.; Renata, H.; Arnold, F.H. Cytochrome P450-catalyzed insertion of carbenoids into N-H bonds. *Chem. Sci.* **2014**, *5*, 598–601. [CrossRef] [PubMed]
16. Tyagi, V.; Fasan, R. Myoglobin-Catalyzed Olefination of Aldehydes. *Angew. Chem. Int. Ed.* **2016**, *55*, 2512–2516. [CrossRef] [PubMed]
17. Sreenilayam, G.; Fasan, R. Myoglobin-catalyzed intermolecular carbene N-H insertion with arylamine substrates. *Chem. Commun.* **2015**, *51*, 1532–1534. [CrossRef]
18. Weissenborn, M.J.; Löw, S.A.; Borlinghaus, N.; Kuhn, M.; Kummer, S.; Rami, F.; Plietker, B.; Hauer, B. Enzyme-catalyzed carbonyl olefination by the *E. coli* protein YfeX in the absence of phosphines. *ChemCatChem* **2016**, *8*, 1636–1640. [CrossRef]
19. Letoffe, S.; Heuck, G.; Delepelaire, P.; Lange, N.; Wandersman, C. Bacteria capture iron from heme by keeping tetrapyrrol skeleton intact. *Proc. Natl. Acad. Sci. USA* **2009**, *106*, 11719–11724. [CrossRef]
20. Dailey, H.A.; Septer, A.N.; Daugherty, L.; Thames, D.; Gerdes, S.; Stabb, E.V.; Dunn, A.K.; Dailey, T.A.; Phillips, J.D. The *Escherichia coli* protein YfeX functions as a porphyrinogen oxidase, not a heme dechelatase. *MBio* **2011**, *2*, e00248-e11. [CrossRef]

21. Liu, X.; Yuan, Z.; Wang, J.; Cui, Y.; Liu, S.; Ma, Y.; Gu, L.; Xu, S. Crystal structure and biochemical features of dye-decolorizing peroxidase YfeX from *Escherichia coli* O157 Asp(143) and Arg(232) play divergent roles toward different substrates. *Biochem. Biophys. Res. Commun.* **2017**, *484*, 40–44. [CrossRef]

22. Hock, K.J.; Knorrscheidt, A.; Hommelsheim, R.; Ho, J.; Weissenborn, M.J.; Koenigs, R.M. Tryptamine synthesis by iron porphyrin catalyzed C-H functionalization of indoles with diazoacetonitrile. *Angew. Chem. Int. Ed.* **2019**, *58*, 3630–3634. [CrossRef]

23. Santos, A.; Mendes, S.; Brissos, V.; Martins, L.O. New dye-decolorizing peroxidases from Bacillus subtilis and *Pseudomonas putida* MET94: Towards biotechnological applications. *Appl. Microbiol. Biotechnol.* **2014**, *98*, 2053–2065. [CrossRef]

24. Yoshida, T.; Sugano, Y. A structural and functional perspective of DyP-type peroxidase family. *Arch. Biochem. Biophys.* **2015**, *574*, 49–55. [CrossRef]

25. Sugano, Y.; Muramatsu, R.; Ichiyanagi, A.; Sato, T.; Shoda, M. DyP, a unique dye-decolorizing peroxidase, represents a novel heme peroxidase family: ASP171 replaces the distal histidine of classical peroxidases. *J. Biol. Chem.* **2007**, *282*, 36652–36658. [CrossRef]

26. Brown, M.E.; Barros, T.; Chang, M.C.Y. Identification and characterization of a multifunctional dye peroxidase from a lignin-reactive bacterium. *ACS Chem. Biol.* **2012**, *7*, 2074–2081. [CrossRef]

27. Ahmad, M.; Roberts, J.N.; Hardiman, E.M.; Singh, R.; Eltis, L.D.; Bugg, T.D. Identification of DypB from *Rhodococcus jostii* RHA1 as a lignin peroxidase. *Biochemistry* **2011**, *50*, 5096–5107. [CrossRef]

28. Rahmanpour, R.; Bugg, T.D. Characterisation of Dyp-type peroxidases from *Pseudomonas fluorescens* Pf-5: Oxidation of Mn(II) and polymeric lignin by Dyp1B. *Arch. Biochem. Biophys.* **2015**, *574*, 93–98. [CrossRef]

29. Pesic, M.; Lopez, C.; Lopez-Santin, J.; Alvaro, G. From amino alcohol to aminopolyol: One-pot multienzyme oxidation and aldol addition. *Appl. Microbiol. Biotechnol.* **2013**, *97*, 7173–7183. [CrossRef]

30. de Gonzalo, G.; Colpa, D.I.; Habib, M.H.; Fraaije, M.W. Bacterial enzymes involved in lignin degradation. *J. Biotechnol.* **2016**, *236*, 110–119. [CrossRef]

31. Yang, C.; Yue, F.; Cui, Y.; Xu, Y.; Shan, Y.; Liu, B.; Zhou, Y.; Lu, X. Biodegradation of lignin by *Pseudomonas* sp. Q18 and the characterization of a novel bacterial DyP-type peroxidase. *J. Ind. Microbiol. Biotechnol.* **2018**, *45*, 913–927. [CrossRef] [PubMed]

32. Habib, M.; Trajkovic, M.; Fraaije, M.W. The biocatalytic synthesis of syringaresinol from 2,6-dimethoxy-4-allylphenol in one-pot using a tailored oxidase/peroxidase system. *ACS Catal.* **2018**, *8*, 5549–5552. [CrossRef] [PubMed]

33. Wasak, A.; Drozd, R.; Struk, Ł.; Grygorcewicz, B. Entrapment of DyP-type peroxidase from *Pseudomonas fluorescens* Pf-5 into Ca-alginate magnetic beads. *Biotechnol. Appl. Biochem.* **2018**, *65*, 238–245. [CrossRef] [PubMed]